NTNU – Trondheim
Norwegian University of
Science and Technology

The linear decision rule approach applied to the hydrothermal generation planning problem

Caroline Tandberg
Signy Elde Vefring

Industrial Economics and Technology Management
Submission date: June 2012
Supervisor: Stein-Erik Fleten, IØT

Norwegian University of Science and Technology
Department of Industrial Economics and Technology Management

Preface

This thesis is the result of the final work done in order to achieve a Master of Science degree with specialization in Managerial Economics and Operation Research, at the Department of Industrial Economics and Technology Management at the Norwegian University of Science and Technology (NTNU), during the spring of 2012.

We would like to thank our supervisor, Professor Stein-Erik Fleten, for advice and support during the report-writing. Special thanks also goes to Erlend Torgnes and Ole Lofsnes at Econ Pöyry for providing both data and guidance. We are particularly grateful for the time PhD candidates Christian Skar and Daniel Haugstvedt have devoted to answer all kinds of questions.

Abstract

We use the linear decision rule approach to develop a model for a stochastic multi-stage generation planning problem in the Nordic region. By developing both the primal and the dual versions of the program, the loss of optimality incurred by the linear decision rule approach can be estimated. Uncertain parameters take values in an uncertainty set defined by upper and lower bounds. Alternative modelling methods for stochastic problems of comparable size and structure either suffer from the curse of dimensionality, or have to rely on unrealistic simplifying assumptions to achieve tractability. We show that the linear decision rule approach gives a good trade-off between tractability and accuracy for a stochastic generation planning problem.

Sammendrag

Ved å anta lineære beslutningsregler utvikler vi en stokastisk fler-stegs modell for planlegging av kraftproduksjon i Norden. Både den primale og den duale versjonen av problemet er implementert. En øvre grense for tapet av optimalitet påført av å begrense beslutningsreglene til å være lineære er beregnet ved å sammenligne den primale objektivverdien med den duale. Usikre parametre kan ta verdier i et sett definert av øvre og nedre grenser. Andre eksisterende løsningsmetoder for å håndtere stokastiske fler-stegs problem får raskt uhåndterbare dimensjoner, eller må benytte seg av urealistiske forenklinger for å oppnå løsbarhet. Vi viser at ved å bruke lineære beslutningsregler på et stokastisk kraftplanleggings-problem, oppnås det en god avveining mellom løsbarhet og presisjon.

Contents

1 Introduction

The perspective of a central planner is used in many power generation planning models for the Nordic region, such as the EMPS and the ECON BID model. This perspective yields the same optimal solution as the solution in a perfect competition market. Since the Nordic region has a functioning deregulated power market, these models are able to give results that correspond to reality.

The task of generation planning is complicated both by the presence of uncertainties and the span in space and time in which the planning takes place. Uncertain factors could include inflow to the reservoirs, fuel prices, capacity limits, consumption and new technology. This implies that multi-stage stochastic modelling of the problem is appropriate.

In stochastic programming the classical approach to solve problems is to approximate the underlying stochastic process of the uncertain parameters to be discrete. The process can then be represented with a finite scenario tree, where each branch represents one possible realization. The solution time of the optimization model scales with the size of the scenario tree, which grows exponentially with the number of time stages. An important issue is therefore to generate scenario trees in a way that gives a good approximate representation of the uncertainty without using a large number of scenarios (Heitsch and Römisch, 2009). However, Kaut and Wallace (2007) state that the ability to guarantee good scenario trees is highly dependent upon the knowledge of the underlying process. As the probability distributions of the uncertain parameters rarely are known, generating good scenario trees can be problematic. Stochastic programming problems are in general hard to solve. Dyer and Stougie (2006) show that two-stage stochastic programming with independently distributed stochastic parameters, following discrete distributions is #P-hard and the multi-stage case is shown to be even harder to solve. According to Shapiro and Nemirovski (2005), stochastic programs are computationally intractable even when medium accuracy solutions are sought. These findings show that it is important to focus on developing tractable methodology, that can reasonably approximate stochastic programs.

Hydrothermal generation planning has been a focus of study in operations research. Stochastic dynamic programming (SDP) has been used to solve the planning problem for the Nordic region, a recent example is given in Wolfgang et al. (2009), where the inflows are modelled as stochastic. The method derives the optimal operating strategy from Bellman's backward recursive relationship (Bellman, 1957), and expected future costs are found at each possible future state. However, the dimensionality of this approach quickly gets out of hand, as discretization of future states is required, and it has limited use for real-size problems. A more re-

cent approach developed by Pereira and Pinto (1991), is known as stochastic dual dynamic programming (SDDP) and uses a decomposition method to handle the multidimensionality of the problem. In this method there is no need for discretization of future states, but both SDP and SDDP use scenarios to model the future, and therefore require scenario generation which in turn can be a demanding task as already discussed.

Our contribution is to show that the linear decision rule (LDR) approach can be beneficially applied to the generation planning problem. The advantage of this approach is that there is no need for state discretization or scenario generation, hence making it an attractive alternative to traditional methods. The general idea of the decision rule approach is to model the decision variables as functions of the realizations of the uncertain parameters. Uncertainties are modelled as continuous random variables that are within upper and lower bounds. The idea itself is old but was recently "resurrected" in Ben-Tal et al. (2004) in the framework of robust optimization. Shapiro and Nemirovski (2005) identifies that the approach scales linearly with the number of time stages, highlighting the benefits of LDR to multi-stage stochastic programming. With the introduction of the dual LDR approximation in Kuhn et al. (2009) it is possible to estimate the loss of accuracy imposed by the LDR approach. The LDR approximation has successfully been used to solve supply chain problems with more than 70 decision stages (Ben-Tal et al., 2005), network design problems involving hundreds of random variables (Atamturk and Zhang, 2007), and robust control problems involving 12 state variables and 20 time stages (Goulart et al., 2008). The approach has also been used in the context of reservoir management as early as in Revelle et al. (1969).

2 Theory

Optimization belongs to the field of applied mathematics and encompasses the use of mathematical models and methods to find the best alternative for a decision maker operating in complex environments. Optimization models are divided in to different classes depending on the functions and variables used to describe the underlying problem. We will focus on the class of *linear programming* (LP) problems, where all functions are linearly dependent on the decision variables and all decision variables are continuous (Lundgren et al., 2010). A typical application of optimization models is on multi-period problems. For these problems the decision maker has to find the values for the decision variables that optimizes the objective function and at the same time satisfies the constraints in each time period. A general linear multi-period program with T periods is can be formulated as

$$\min z = \sum_{t=1}^{T} \boldsymbol{c}_t^\top \boldsymbol{x}_t \tag{2.1a}$$

$$\text{s.t.} \quad \sum_{s=1}^{T} \boldsymbol{A}_{ts} \boldsymbol{x}_s \geq \boldsymbol{b}_t \tag{2.1b}$$

$$\boldsymbol{x}_t \geq \boldsymbol{0}, \tag{2.1c}$$

in which the $\boldsymbol{x}_t$ vectors of size n represent the decisions taken in time period t. The objective function coefficients $\boldsymbol{c}_t$ are vectors of size n and exist for each period t. The number of constraint matrices $\boldsymbol{A}_{ts}$ of size $m \times n$ is $T \times T$ such that period-t constraints can include decision variables from other time periods. The right-hand side vector $\boldsymbol{b}_t$ is of size m.

To describe a problem as exact as possible, parameters $\boldsymbol{A}_{ts}$, $\boldsymbol{b}_t$ and $\boldsymbol{c}_t$ need to be carefully determined. Some parameters might be time-consuming to determine due to the complexity of the problem, an example being the variable cost of production. Other parameters might not be possible to determine with certainty at all, such as future demand. Because the future is in fact uncertain, most real life problems include some parameters of this last type. It is well documented in theory and practice that disregarding or underestimating uncertainty is a common mistake that often results in severely suboptimal decisions (Kuhn et al., 2011). *Stochastic* models account for uncertainty in contrast to *deterministic* models which assume that all parameters can be stated with certainty. As most real life problems are affected by uncertainty of some form, the modelling potential for stochastic programs is significant.

When uncertainty is introduced in an optimization model, the timing of the decisions relative to the timing of new information must be specified. Decisions taken after observing the uncertain parameters offers an opportunity to adapt to the received information, and are called recourse decisions (Higle, 2005). A *stage* is commenced when new information is observed. Stages define the basic structure of stochastic problems, as this is the only time it is meaningful to make new decisions. Multi-stage recourse models describe problems where there is a sequence of uncertain parameters being revealed and associated recourse decisions being made. *Nonanticipativity constraints* are included in multi-stage models to ensure that decisions taken at a specific stage only rely on information available at this stage. The multi-stage recourse problem has attracted a lot of attention as its structure is applicable to a large class of practical problems (Chen et al., 2008).

2.1 The decision rule approach

Recourse decisions can be modelled as decision rules. In this section, we present a general formulation for a decision making problem under uncertainty with T stages. The structure and notation is the same as in Kuhn et al. (2011) and will be used throughout this text. We are consistent in the use of bold for matrices and vectors.

The uncertain parameters observed in any stage t are noted $\boldsymbol{\xi}_t \in \mathbb{R}^{k_t}$,where k_t is the number of uncertain parameters observed in stage t. The uncertainty set Ξ represents the range of all values $\boldsymbol{\xi}$ can adapt, and is assumed to be a bounded polyhedron of the form

$$\Xi = \big[\boldsymbol{\xi} \in \mathbb{R}^k : \boldsymbol{W}\boldsymbol{\xi} \geq \boldsymbol{h}\big], \tag{2.2}$$

for some $\boldsymbol{W} \in \mathbb{R}^{l \times k}$ and $\boldsymbol{h} \in \mathbb{R}^l$. Naturally decisions taken at stage t can only be based on the already observed parameters $\boldsymbol{\xi}_1, \boldsymbol{\xi}_2, \ldots, \boldsymbol{\xi}_t$ and not on future observations $\boldsymbol{\xi}_{t+1}, \boldsymbol{\xi}_{t+2}, \ldots, \boldsymbol{\xi}_T$. Decisions are based on the whole history of observations, i.e. $\boldsymbol{x}_t(\boldsymbol{\xi}_1, \boldsymbol{\xi}_2, \ldots, \boldsymbol{\xi}_t) \in \mathbb{R}^{n_t}$, in which n_t represents the number of decisions made in stage t. Requiring that $\boldsymbol{x}_t$ depends solely on $\boldsymbol{\xi}^t$ reflects the nonantcipative nature of the problem. For simplicity, the history of observations is defined as $\boldsymbol{\xi}^t = (\boldsymbol{\xi}_1, \boldsymbol{\xi}_2, \ldots, \boldsymbol{\xi}_t) \in \mathbb{R}^{k^t}$, where $k^t = \sum_{s=1}^{t} k_s$ and represents the total number of observed parameters up to stage t. Finally, $\boldsymbol{\xi} = \boldsymbol{\xi}^T$ and $k = k^T$, representing the complete set of the uncertain parameters and the total number of observed parameters respectively.

By using this general notation, we can explicitly include uncertainty in the general linear multi-stage problem presented in Equation (2.1). We will focus on the case of fixed recourse, meaning that the constraint matrices $\boldsymbol{A}_{ts}$ are independent of $\boldsymbol{\xi}$.

The case of random recourse is more intricate and is investigated in Kuhn et al. (2009). A stochastic problem will often have some decisions and constraints not affected by uncertainty. To make it convenient to include deterministic decisions and constraints we will require that the first element of all scenarios $\boldsymbol{\xi}_1$ is equal to 1. This requirement will not cause any loss of generality and has notational advantage.

The general formulation for a decision making problem under uncertainty with T stages can be formulated with decision rules in the following way:

$$\begin{aligned} &\text{minimize } \mathbb{E}_{\xi}\Big(\sum_{t=1}^{T} \boldsymbol{c}_t(\boldsymbol{\xi_t})^\top \boldsymbol{x_t}(\boldsymbol{\xi}_t)\Big) \qquad (\mathcal{P}) \\ &\left.\begin{aligned} \text{subject to } \mathbb{E}_{\boldsymbol{\xi}}\Big(\sum_{s=1}^{T} \boldsymbol{A}_{ts}\boldsymbol{x}_s(\boldsymbol{\xi}^s)\Big|\boldsymbol{\xi}^t\Big) &\geq \boldsymbol{b}_t(\boldsymbol{\xi}^t), \\ \boldsymbol{x}_t(\boldsymbol{\xi}^t) &\geq \mathbf{0} \end{aligned}\right\} \quad \forall t \in \mathcal{T} \quad \forall \boldsymbol{\xi} \in \Xi \end{aligned}$$

In the formulation above, $\mathbb{E}_{\xi}(\cdot)$ denotes expectation with respect to the random parameters $\boldsymbol{\xi}$ and $\mathcal{T}$ is the set $(1, \ldots, T)$ of time stages.

The general decision problem formulated in $\mathcal{P}$ provides considerable modelling flexibility. In Kuhn et al. (2011) it is shown how the problem $\mathcal{P}$ encapsulates deterministic and multi-stage stochastic linear programs, robust optimization problems and tight convex approximation of chance-constrained programs as a special case.

The uncertainty set can contain infinitely many scenarios $\boldsymbol{\xi}$. All of the stage t decisions, $\boldsymbol{x}_t(\boldsymbol{\xi}^t)$, are parametrised in $\boldsymbol{\xi}^t$. Each $\boldsymbol{\xi}^t$ corresponds to one scenario $\boldsymbol{\xi}$ which results in infinitely many decision variables. A similar argument can be deducted for the constraints. The stage-t constraints are conditioned on the observation history $\boldsymbol{\xi}^t$ because $\mathbb{E}(\cdot|\boldsymbol{\xi}^t)$ is the conditional expectation with respect to $\boldsymbol{\xi}$ given $\boldsymbol{\xi}^t$. This implies that also the stage-t constraints are parametrised in $\boldsymbol{\xi}^t$ and that there will be infinitely many constraints when there are infinitely many $\boldsymbol{\xi}$ in Ξ. An infinite number of decision variables and constraints makes the program $\mathcal{P}$ severely computationally intractable.

2.2 Linear decision rules

A tractable approximation for problem $\mathcal{P}$ is obtained by restricting the space of decision rules to those that exhibit a linear dependence on the observation history

$\boldsymbol{\xi}^t$.

For the further argumentation we define the truncation operator $\boldsymbol{P}_t : \mathbb{R}^k \longrightarrow \mathbb{R}^{k^t}$ through $\boldsymbol{P}_t\boldsymbol{\xi} = \boldsymbol{\xi}^t$. Restricting the decision rules to be linear then amounts to setting

$$\boldsymbol{x}_t(\boldsymbol{\xi}^t) = \boldsymbol{X}_t\boldsymbol{\xi}^t = \boldsymbol{X}_t\boldsymbol{P}_t\boldsymbol{\xi} \tag{2.3}$$

where $\boldsymbol{X} \in \mathbb{R}^{n_t \times k^t}$. The objective function coefficients and the right hand side vectors are linear functions of the observation history, and can be defined as $\boldsymbol{c}_t(\boldsymbol{\xi}^t) = \boldsymbol{C}_t\boldsymbol{\xi}^t = \boldsymbol{C}_t\boldsymbol{P}_t\boldsymbol{\xi}$ for some $\boldsymbol{C}_t \in \mathbb{R}^{n_t \times k^t}$ and $\boldsymbol{b}_t(\boldsymbol{\xi}^t) = \boldsymbol{B}_t\boldsymbol{\xi}^t = \boldsymbol{B}_t\boldsymbol{P}_t\xi$ for some $\boldsymbol{B}_t \in \mathbb{R}^{m_t \times k^t}$. This is a nonrestrictive assumption since we are free to redefine $\boldsymbol{\xi}$ such that it contains $\boldsymbol{c}_t(\boldsymbol{\xi}^t)$ and $\boldsymbol{b}_t(\boldsymbol{\xi}^t)$ as subvectors (Kuhn et al., 2009). For simplicity we define $m = \sum_{t=1}^{T} m_t$, and $n = \sum_{t=1}^{T} n_t$, as the total number of constraints and variables respectively.

Substituting the linear decision rules and the expressions for $\boldsymbol{c}_t(\boldsymbol{\xi}^t)$ and $\boldsymbol{b}_t(\boldsymbol{\xi}^t)$ into $\mathcal{P}$ yields the following problem.

$$\begin{aligned} &\text{minimize } \mathbb{E}_\xi\Big(\sum_{t=1}^{T}(\boldsymbol{C}_t\boldsymbol{P}_t\boldsymbol{\xi})^\top \boldsymbol{X}_t\boldsymbol{P}_t\boldsymbol{\xi}\Big) && (\mathcal{P}^u) \\ &\left.\begin{aligned} \text{subject to } \mathbb{E}_\xi\Big(\sum_{s=1}^{T}\boldsymbol{A}_{ts}\boldsymbol{X}_s\boldsymbol{P}_s\boldsymbol{\xi}\Big|\boldsymbol{\xi}^t\Big) &\geq \boldsymbol{B}_t\boldsymbol{P}_t\boldsymbol{\xi}, \\ \boldsymbol{X}_t\boldsymbol{P}_t\boldsymbol{\xi} &\geq \boldsymbol{0}, \end{aligned}\right\} && \forall t \in \mathcal{T} \quad \forall \boldsymbol{\xi} \in \Xi \end{aligned}$$

To ensure that the linear decision rule approximation will convert to a tractable program, we require the conditional expectations $\mathbb{E}_\xi(\boldsymbol{\xi}|\boldsymbol{\xi}^t)$ to be linear in $\boldsymbol{\xi}^t$ (Kuhn et al., 2009). In other words there should exist matrices $\boldsymbol{M}_t \in \mathbb{R}^{k \times k^t}$ such that $\mathbb{E}_\xi(\boldsymbol{\xi}|\boldsymbol{\xi}^t) = \boldsymbol{M}_t\boldsymbol{\xi}^t$ for all $\boldsymbol{\xi} \in \Xi$. If, for example, the parameters $\boldsymbol{\xi}_t$ are mutually independent or if the process of the random parameters belong to the class of autoregressive moving-average models, this requirement is automatically satisfied (Kuhn et al., 2011).

The problem can be simplified and re-expressed in terms of $\boldsymbol{M}_t$, and the second order moment matrix of the random parameters $\boldsymbol{M} \in \mathbb{R}^{k \times k}$ defined by $\boldsymbol{M} = \mathbb{E}(\boldsymbol{\xi}\boldsymbol{\xi}^t)$. The steps of these algebraic manipulations are stated in Kuhn et al. (2011), and the resulting reformulation of $\mathcal{P}^u$ is $\bar{\mathcal{P}}^u$.

$$\begin{aligned}
&\text{minimize} \sum_{t=1}^{T} \operatorname{Tr}(\boldsymbol{P}_t \boldsymbol{M} \boldsymbol{P}_t^\top \boldsymbol{C}_t^\top \boldsymbol{X}_t) && (\bar{\mathcal{P}}^u)\\
&\text{subject to } \Big(\sum_{s=1}^{T} \boldsymbol{A}_{ts} \boldsymbol{X}_s \boldsymbol{P}_s \boldsymbol{M}_t \boldsymbol{P}_t - \boldsymbol{B}_t \boldsymbol{P}_t \Big) \boldsymbol{\xi} \geq \boldsymbol{0}, \\
&\qquad\qquad \boldsymbol{X}_t \boldsymbol{P}_t \boldsymbol{\xi} \geq \boldsymbol{0}, \end{aligned} \Bigg\} \quad \forall t \in \mathcal{T} \quad \forall \boldsymbol{\xi} \in \Xi$$

We can see from the new formulation that the decision variables no longer are parametrised in $\boldsymbol{\xi}$. By restricting the decision rules to be linear, the number of decision variables equals the finite number of elements in the matrices $\boldsymbol{X}_1, \ldots, \boldsymbol{X}_T$. The problem is, however, still not suitable for numerical solution due to the infinite number of constraints. Robust optimization techniques offer a proposition to reformulate the $\boldsymbol{\xi}$-dependent constraints in terms of a finite number of linear constraints. We will only show the final result of this transformation without repeating the involved manipulations, the proposition used can be found in Kuhn et al. (2011).

$$\begin{aligned}
&\text{minimize} \sum_{t=1}^{T} \operatorname{Tr}(\boldsymbol{P}_t \boldsymbol{M} \boldsymbol{P}_t^\top \boldsymbol{C}_t^\top \boldsymbol{X}_t) && (\mathcal{P}^U)\\
&\text{subject to } \Big(\sum_{s=1}^{T} \boldsymbol{A}_{ts} \boldsymbol{X}_s \boldsymbol{P}_s \boldsymbol{M}_t \boldsymbol{P}_t - \boldsymbol{B}_t \boldsymbol{P}_t \Big) = \boldsymbol{\Lambda}_t \boldsymbol{W}, \\
&\qquad\qquad \boldsymbol{X}_t \boldsymbol{P}_t = \boldsymbol{\Gamma}_t \boldsymbol{W}, \\
&\qquad\qquad \boldsymbol{\Lambda}_t \boldsymbol{h} \geq \boldsymbol{0}, \\
&\qquad\qquad \boldsymbol{\Gamma}_t \boldsymbol{h} \geq \boldsymbol{0}, \\
&\qquad\qquad \boldsymbol{\Lambda}_t, \boldsymbol{\Gamma}_t \geq \boldsymbol{0} \end{aligned} \Bigg\} \quad \forall t \in \mathcal{T}$$

The decision variables in $\mathcal{P}^U$ are the elements of matrices $\boldsymbol{X}_t \in \mathbb{R}^{n_t \times k^t}$, $\boldsymbol{\Lambda}_t \in \mathbb{R}^{m_t \times l}$ and $\boldsymbol{\Gamma}_t \in \mathbb{R}^{n_t \times l}$ for $t = 1, \ldots, T$. The decision variables $\boldsymbol{\Lambda}_t$ and $\boldsymbol{\Gamma}_t$ can be described as support variables to ensure feasibility for all $\boldsymbol{\xi} \in \Xi$. Both objective function and constraints are linear in the decision variables and the dimensions of the problem is finite. The problem described in $\mathcal{P}^U$ can thus be solved efficiently with off-the-shelf LP solvers.

The size of the problem $\mathcal{P}^U$ grows polynomially in k, l, m and n. These numbers increase linearly with T, making the size of $\mathcal{P}^U$ scale only quadratically with the number of decision stages.

2.3 Approximation error

The massive reduction of computational complexity incurred by restricting the decision rules to be linear, necessarily comes at the loss of optimality. With this restriction we underestimate the decision makers flexibility, as decision rules in reality can take any functional form. The difference between the objective values of the LDR approximation and the exact problem, $\Delta^U = \min\mathcal{P}^U - \min\mathcal{P}$, is the loss of optimality. As $\mathcal{P}^U$ is a restriction of a minimization problem, Δ^U is necessarily non-negative making the objective value of $\mathcal{P}^U$ an upper bound for the objective value of $\mathcal{P}$.

The calculation of Δ^U requires the solution of $\mathcal{P}$ itself which, as we know, is unattainable. We can find a lower bound for the optimal objective value of $\mathcal{P}$ by solving the associated dual program $\mathcal{D}$. Unfortunately the program $\mathcal{D}$ is as intractable as $\mathcal{P}$ due to the infinite number of constraints and decision variables. Using the same arguments as for the primal problem $\mathcal{P}$, the dual problem $\mathcal{D}$ can be re-formulated as a finite linear program by restricting the dual decision variables to be linear functions of the observation history $\boldsymbol{\xi}^t$. The steps of the re-formulation can be studied in Kuhn et al. (2011), and the final formulation is

$$
\begin{array}{ll}
\text{maximize} & \displaystyle\sum_{t=1}^{T} \mathrm{Tr}(\boldsymbol{P}_t \boldsymbol{M} \boldsymbol{P}_t^\top \boldsymbol{B}_t^\top \boldsymbol{Y}_t) \qquad (\mathcal{D}^L) \\
\text{subject to} & \left.\begin{array}{r}
\displaystyle\Big(\sum_{s=1}^{T} \boldsymbol{A}_{st}^\top \boldsymbol{Y}_s \boldsymbol{P}_s \boldsymbol{M}_t \boldsymbol{P}_t - \boldsymbol{C}_t \boldsymbol{P}_t\Big) = \boldsymbol{\Phi}_t \boldsymbol{W}, \\
\boldsymbol{Y}_t \boldsymbol{P}_t = \boldsymbol{\Psi}_t \boldsymbol{W}, \\
\boldsymbol{\Phi}_t \boldsymbol{h} \leq \boldsymbol{0}, \\
\boldsymbol{\Psi}_t \boldsymbol{h} \geq \boldsymbol{0}, \\
\boldsymbol{\Phi}_t, \boldsymbol{\Psi}_t \leq \boldsymbol{0},
\end{array}\right\} \quad \forall t \in \mathcal{T}
\end{array}
$$

The decision variables in $\mathcal{D}^L$ are the elements of matrices $\boldsymbol{Y}_t \in \mathbb{R}^{m_t \times k^t}$, $\boldsymbol{\Phi}_t \in \mathbb{R}^{n_t \times l}$ and $\boldsymbol{\Psi}_t \in \mathbb{R}^{m_t \times l}$ for $t \in \mathcal{T}$. The matrices $\boldsymbol{\Phi}_t$ and $\boldsymbol{\Psi}_t$ are analogue to the primal matrices $\boldsymbol{\Lambda}_t$ and $\boldsymbol{\Gamma}_t$, while the matrices $\boldsymbol{Y}_t$ contain the coefficients in the dual linear decision rules. As both objective function and constraints are linear in the decision variables and the dimensions of the problem are finite, the problem described in $\mathcal{D}^L$ can just like the primal version described in $\mathcal{P}^U$ be solved efficiently.

The dual approximation error can be defined as $\Delta^L = \min\mathcal{D}^L - \min\mathcal{D}$ and is necessarily non-negative as $\mathcal{D}^L$ is a restriction of a maximization problem. Although

neither Δ^L or Δ^U can be calculated, the joint primal and dual approximation error Δ = min $\mathcal{P}^U$ - max $\mathcal{D}^L$ can be found by finding solutions to two tractable programs.

$$\begin{aligned}\Delta &= \min\mathcal{P}^U - \max\mathcal{D}^L \\ &= \min\mathcal{P}^U - \min\mathcal{P} + \min\mathcal{P} - \max\mathcal{D} + \max\mathcal{D} - \max\mathcal{D}^L \\ &= \Delta^U + \min\mathcal{P} - \max\mathcal{D} + \Delta^L \\ &\geq \Delta^U + \Delta^L \end{aligned} \tag{2.4}$$

The last equality in (2.4) follows from weak duality, and show that Δ constitutes an upper bound on both Δ^U and Δ^L. A large Δ thus indicates the possibility for a large approximation error, and corresponding low accuracy. Similarly, a small Δ indicates a small approximation error and high accuracy.

2.4 Stage aggregation

Many models require a large number of time stages to describe the underlying problem in a satisfactory way. The size of LDR models grows only quadratically with the number of time stages, but also for this approach the computation time will eventually become unacceptable. To be able to efficiently solve problems with a large number of time stages, stage aggregation can be applied. Rocha and Kuhn (2012) use the combination of LDR and stage aggregation on a portfolio optimization problem for an electricity retailer in a deregulated electricity market.

The idea of stage aggregation is to reduce the number of times the decision maker receives new information, thus reducing the actual number of stages in the problem. To do so the planning horizon T is subdivided into a number of *macroperiods* $s \in (1, \ldots, S)$, and the problem is re-formulated such that the decision maker only receives new information at the start of a new macroperiod. We let t_s denote the first time stage belonging to macroperiod s. All decisions taken within macroperiod s are based on the observation history $\boldsymbol{\xi}^{t_s}$. From Section 2.1 we recall that k_t defines the number of parameters observed in stage t. When stage aggregation is used, $k_t = 0$ for all periods except the first in each macroperiod.

3 Application: Generation planning in a hydrothermal system

Our application of the LDR approach is on a hydrothermal generation planning problem of the Nordic power system. From the point of view of a system-wide planner, the objective is to determine generation targets for each power plant and transmission targets for each power line such that the total expected costs are minimized. These costs consist of fuel costs for thermal units together with purchase costs from neighboring regions. Demand in each area has to be satisfied in all time periods, and the transmission and generation must not override their capacity limits. The Nordic system is dominated by hydropower generation where reservoirs provide a means to store energy. Having this flexibility is valuable because it makes it possible to distribute the use of "free" hydro generation to time periods with high thermal generation cost. Availability of the water is limited by the upper and lower limits of the reservoir, and the inflow. This imposes a time dependence on the operating decisions, where a decision today affects the operating costs in the future.

In our application, the planning horizon is 60 weeks, and the time resolution is weekly. The areas are aggregated into the four Nordic countries Norway, Sweden, Finland and Denmark, and all data are given as aggregated for each of these areas. Denmark is the only area without hydropower. There are seven generator types and 18 transmission lines, in which ten are between areas, and eight connect the areas to outside regions. We define an *area* as being inside the model, and an *outside region* if it is outside the model and not part of the optimization process. Coupling with the outside regions is done on the basis of power prices, and the regions in the model are Germany, Poland and the Netherlands. Figure 3.1 gives a visualization of the problem modelled.

In Section 3.1 a deterministic model is developed, and this model is then used as a basis for the LDR model developed in Section 3.3. In the LDR approach, uncertainties in fuel prices and inflow are taken into account.

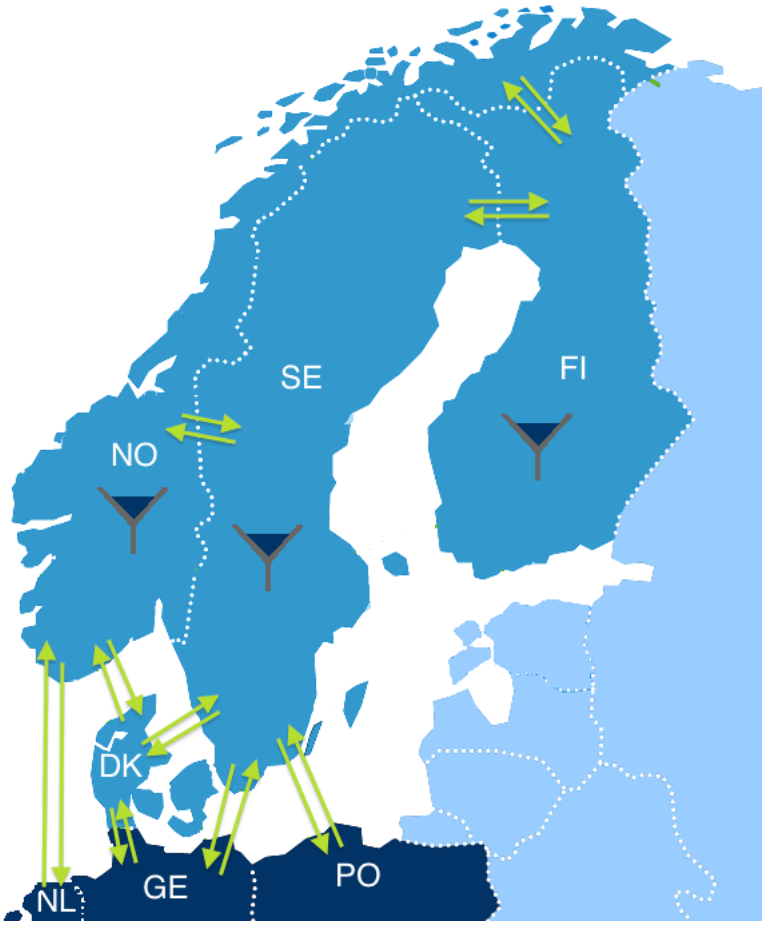

Figure 3.1: Picture of the Nordic power system with connections to Europe.

3.1 Deterministic model

The complete mathematical formulation of the deterministic generation planning model is given in this section.

Sets and indices

$\mathcal{A}$: set of areas, indexed by $i \in (1, \ldots, A)$
$\mathcal{T}$: set of time periods, indexed by $t \in (1, \ldots, T)$
$\mathcal{L}$: set of transmission lines, indexed by $l \in (1, \ldots, L)$
$\mathcal{J}$: set of generator types, indexed by $j \in (1, \ldots, J)$
$\mathcal{O}$: set of outside regions, indexed by $o \in (1, \ldots, O)$
$\mathcal{H}$: set of hydro-producing areas ($\mathcal{H} \subset \mathcal{A}$)

Parameters

γ :	percentage line loss
C_{tj} :	running cost of generator type j in time period t [€/MWh]
D_{ti} :	demand in area i in period t [MWh/week]
TC_l :	transmission capacity of flow in line l [MWh/week]
GC_{ji} :	capacity of generator type j in area i [MWh/week]
I_{ti} :	inflow in area i in period t [MWh/week]
R_i^{Max} :	reservoir maximum in area i [MWh]
R_i^{Min} :	reservoir minimum in area i [MWh]
R_i^{Start} :	start reservoir level in area i [MWh]
R_i^{End} :	minimum end reservoir level in area i [MWh]
ToA_l :	the area/region that line l goes to
FrA_l :	the area/region that line l goes from
P_{to} :	power prices in outside region o in time period t [€/MWh]

Variables

g_{tji} :	generation of generator type j in area i in time period t [MWh/week]
b_{tl} :	flow in transmission line l in time period t [MWh/week]

Mathematical formulation The mathematical formulation of the generation planning problem stated below has the same underlying structure as the general multi-period problem (2.1).

$$min \sum_{t \in T} \Big[\sum_{i \in A} \sum_{j \in J} C_{tj} g_{tji} \tag{3.1a}$$

$$+ \sum_{o \in O} \Big(\sum_{\substack{l \in L: \\ ToA_l = o}} P_{to} b_{tl} - \sum_{\substack{l \in L: \\ FrA_l = o}} P_{to} b_{tl} \Big) \Big], \tag{3.1b}$$

for all timeperiods t $\in \mathcal{T}$ subject to:

$$\sum_{j\in J} g_{tji} + \sum_{\substack{l\in L:\\ ToA_l=i}} b_{tl}(1-\gamma) - \sum_{\substack{l\in L:\\ FrA_l=i}} b_{tl} \geq D_{ti}, \qquad \forall i \in \mathcal{A} \qquad (3.2)$$

$$\sum_{s=1}^{t-1} g_{s,1,i} \geq R_i^{Start} - R_i^{Max} + \sum_{s=1}^{t-1} I_{si}, \quad \forall i \in \mathcal{H} \qquad (3.3)$$

$$-\sum_{s=1}^{t-1} g_{s,1,i} \geq R_i^{Min} - R_i^{Start} - \sum_{s=1}^{t-1} I_{si}, \quad \forall i \in \mathcal{H} \qquad (3.4)$$

$$-g_{tji} \geq -GC_{ji}, \qquad \forall i \in \mathcal{A}, \quad \forall j \in \mathcal{J} \qquad (3.5)$$

$$-b_{tl} \geq -TC_l, \qquad \forall l \in \mathcal{L} \qquad (3.6)$$

$$g_{tji}, b_{tl} \geq 0, \qquad \forall i \in \mathcal{A}, \quad \forall j \in \mathcal{J}, \forall l \in \mathcal{L} \qquad (3.7)$$

The objective of the planning problem is to minimize total generation cost in all areas and time periods, as seen in (3.1a). In addition, there is negative cost when selling power to outside regions, and a positive cost when buying as seen in the part (3.1b). Constraint (3.2) is the power balance constraint, ensuring that demand is covered in all areas and in all time periods. The demand is covered by the areas own generation, plus import and less export. The reservoirs in each area need to be within their minimum and maximum levels. Reservoir level in one period is equal to the reservoir level in the previous period plus the inflow minus the hydro-generation as seen in the water balance constraints (3.3) and (3.4). Generation must be nonnegative and within the capacity limits in each area and for each generator type. The flow in each powerline must also be nonnegative, and within the transmission capacity of the given line. These variable requirements are represented by the constraints (3.5) - (3.7).

To ensure that the reservoirs levels at the end of period T do not fall below a set target, an end reservoir requirement is specified with additional constraints:

$$\sum_{s\in\mathcal{T}} g_{s,1,i} \geq R_i^{Start} - R_i^{Max} + \sum_{s\in\mathcal{T}} I_{si}, \quad \forall i \in \mathcal{H} \qquad (3.8)$$

$$-\sum_{s\in\mathcal{T}} g_{s,1,i} \geq R_i^{End} - R_i^{Start} - \sum_{s\in\mathcal{T}} I_{si}, \quad \forall i \in \mathcal{H} \qquad (3.9)$$

3.2 Data

The modelling period is defined as being the 60 weeks from January 2008–March 2009. In this section, all data used in the model is defined.

Generation The set of generators are:

$$\mathcal{J} = \{\text{Hydro}, \quad \text{Nuclear}, \quad \text{CoalCondensing}, \quad \text{CoalExtraction}, \\ \text{GasExtraction}, \quad \text{CCGT}, \quad \text{GasTurbine}\}$$

Generator types 3 and 4 are fueled by coal, and types 5, 6 and 7 are fueled by gas. CCGT stands for combined cycle gas turbine. Generation capacities are constant for the whole of the modelling period, and are seen in Table 3.1. The data is from Nordel and Thema Consulting group.

Table 3.1: Generator capacities in all areas [GWh/week]

	NO	SE	FI	DK
Hydro	4951.6	2720.8	520.3	0
Nuclear	0	1501.6	444.5	0
CoalCondensing	0	0	279.6	68.7
CoalExtraction	0	0	154.4	713.2
GasExtraction	0	0	30.4	246.5
CCGT	70.6	0	0	80.1
GasTurbine	0	692.7	90.4	98.8

The following equation was used to calculate the generation cost of the generator types in all time periods:

$$C_{tj} = \frac{PF_{tj}}{E_f \eta_j} + V_j + \frac{PC_t N_f}{\eta_j} \tag{3.10}$$

where,

C_{tj} : running cost of generator type j in time period t [€/MWh]
PF_{tj} : fuel price for generator j in time period t [€/ton]
PC_t : price of CO_2-quota in time period t [€/ton]
N_f : CO_2 content in fueltype f [MWh/ton]
E_f : energy content in fueltype f [MWh/ton]
V_j : variable operating cost of generator type j [€/MWh]
η_j : efficiency of generator j

We further define PK_t as the coal price and PG_t as the gas price in each period. Table 3.2 shows the relevant characteristics for the different generator types. Hydro- and nuclear generators are modelled using fixed variable production costs, and the variable cost for the gas turbine reflects the cost for staying idle. There are no start-up costs for the generators, and the generator up-time is 168 hours per week. The data is from Thema Consulting Group.

Table 3.2: Fuel type, efficiency and variable cost of generator types.

Generator type	Fuel type	η_j [%]	V_j [€/MWh]
Hydro	n/a	100	0.0
Nuclear	n/a	100	15.0
CoalCondensing	Coal	42	1.5
CoalExtraction	Coal	41	1.5
GasExtraction	Gas	39	1.5
CCGT	Gas	54	1.5
GasTurbine	Gas	35	25.0

Table 3.3 shows energy content and CO_2 content for the fuels. Data is from Econ Pöyry.

Table 3.3: Energy and CO_2 content for coal and gas.

Fuel type	N_f [ton/MWh]	E_f [MWh/ton]
Coal	0.34	7.17
Gas	0.20	13.33

The expected prices for coal and gas are found by using the weekly average prices from the years 2000–2010. The data for the coal prices are from McCloskey, and for the gas prices the data is from Nord Pool Gas and Reuter Ecowin. The CO_2-quota prices are from the actual modelling period, and is from NASDAQ OMX Commodities Europe.

Transmission The power lines connecting the areas together and coupling the Nordic areas with the outside regions have constant capacity and no ramping constraints. The losses are one percent of the transmitted amount. Table 3.4 gives the capacities, and the data is from Econ Pöyry.

Table 3.4: Transmission capacities and destinations of power lines.

From area	To area	TC_l [GWh/week]
NO	SE	596.4
NO	DK	159.6
NO	FI	16.8
SE	NO	655.2
SE	DK	332.6
SE	FI	344.4
DK	NO	159.6
DK	SE	409.9
FI	NO	16.8
FI	SE	277.2
NO	NL	117.6
SE	GE	100.8
SE	PO	100.8
DK	GE	350.3
GE	SE	100.8
GE	DK	260.4
NL	NO	117.6
PO	SE	100.8

Demand Generation from CHP and wind is modelled as fixed parameters as they in reality are highly dependable on factors not included in this model. In the demand data used the generation from CHP and wind in the actual planning period is subtracted from the consumption in the same period. The demand data is retrived from Nord Pool Spot and shown in Figure 3.2.

Inflow Data for expected weekly inflows to reservoirs are derived by taking the average inflow of the corresponding week in the period 1995–2010. The inflow data is shown in Figure 3.3, where it can be seen that the inflow is greatest in Norway which is natural as it is the country with the highest reservoir capacity in the Nordics. Furthermore, the inflow is higher in spring and summer, because in

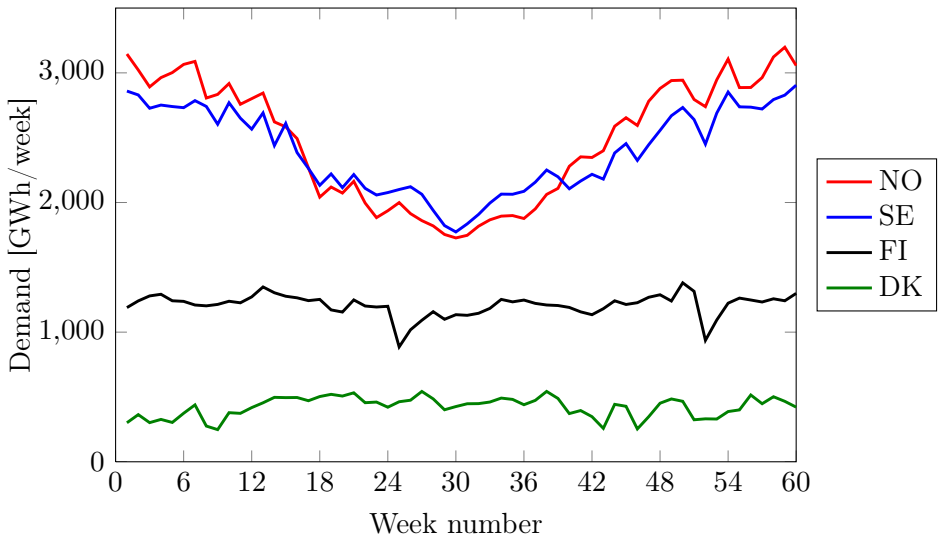

Figure 3.2: Demand in all areas with CHP and wind production subtracted.

addition to the precipitation falling as rain, the snow reservoirs are melting. The data is from Vattenfall and Nord Pool Spot.

Reservoir data The expected reservoir level at the end of the planning horizon should be higher or equal to the specified end reservoir level, R_i^{End}. The start and end reservoir values are average values for the corresponding week during the years 2000–2010. During this period, the capacity has been near constant. Reservoir data used in the model is given in Table 3.5 where R_i^{End} is given for $T = 60$.

Table 3.5: Reservoir data for all hydro producing areas [GWh]

	NO	SE	FI
R_i^{Max}	81888	33758	5530
R_i^{Min}	10000	10000	1000
R_i^{Start}	54515	19975	3412
R_i^{End}	37155	11506	2363

Outside region power prices The weekly average power prices in the outside regions during the modelling period are used in the model. The power price data in these regions are from the power exchanges in the respective countries.

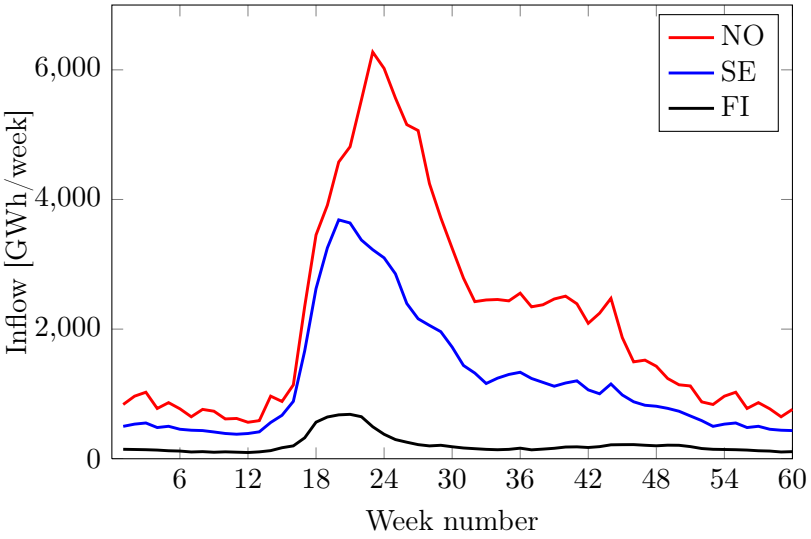

Figure 3.3: Expected inflow in all hydro-producing areas.

3.3 The LDR model

We have applied the LDR framework described in Section 2.2 to the generation planning problem outlined in Section 3.1. We have used matrix formulation and the reader is referred to Guslitser (2002) for a LDR inventory problem given in summation form. Our procedure in implementing the generation planning problem has been to generate the matrices for problem $\mathcal{P}^U$ in MATLAB. MATLAB is then used to perform necessary matrix calculations and format the resulting constraints and objective function to text-files with MOSEL-code. These text files are then included in XPRESS^{MP} which solves the program. The work flow is illustrated in Figure 3.4. In this section, we will explain the contents of these matrices as fully as we find necessary in order for the reader to understand the implementation. The MATLAB-scripts together with the MOSEL-code and data files can be found at the following webpage: http://folk.ntnu.no/vefring. The deterministic model is also implemented and attached here.

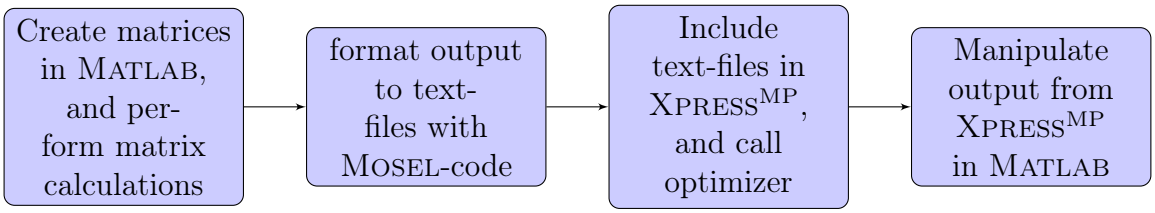

Figure 3.4: Flowchart showing the modelling process.

Uncertain parameters The inflows to hydro-producing areas and fuel prices for all time stages make up the set of uncertain parameters in $\boldsymbol{\xi}$. All parameters are modelled as mutually independent random variables with a uniform distribution between upper and lower bounds. The number of uncertain parameters revealed in each time period, k_t, is equal to five; the inflow to each of the three hydro-producing areas, the price of gas and the price of coal. Decisions are made at the beginning of each week, and we are able to make these decisions on the basis of the inflows observed up until the previous week and the fuel prices observed up until the present week. This is an appropriate representation of reality as a planner would know the price in the current period, whereas he would only know the actual inflow after it has been observed. The uncertain parameters revealed at stage t are then:

$$\boldsymbol{\xi}_t = \begin{bmatrix} I_{t-1,1} \\ I_{t-1,2} \\ I_{t-1,3} \\ PK_t \\ PG_t \end{bmatrix}.$$

The expected values of the uncertain parameters are known in the beginning of the planning period, and is denoted with an asterisk. I^*_{ti} is the expected inflow, PK^*_t is the expected coal price and PG^*_t is the expected gas price. The fuel prices affect the generation costs according to Equation (3.10).

Support estimation The upper and lower bounds on the uncertain parameters is defined by a uncertainty level θ. For example, inflow is described as:

$$I_{ti} \in [I^*_{ti}(1-\theta^I), I^*_{ti}(1+\theta^I)] \qquad t \in \mathcal{T}, i \in \mathcal{A} \tag{3.11}$$

Bounds on the possible realizations of the uncertain fuel prices are found in the same way with θ^{PK} and θ^{PG} defining the uncertainty levels of coal and gas respectively. Uncertainty levels can be calculated so as to cover specified proportions of the mass of the underlying probability distribution as in Rocha and Kuhn (2012). Part of our experiments has been to assess the influence of different uncertainty levels θ, and having a variety of uncertainty levels have therefore been more important then the numeric values of these levels. As we describe the support using a percentage of the expected value, the uncertainty is naturally larger in absolute values when the expected values are larger. This can be seen in Figure 3.5, where the expected inflow in Sweden is plotted with the upper and lower bounds for $\theta^I = 0.2$. A sample realization of the actual inflow is also shown in the figure.

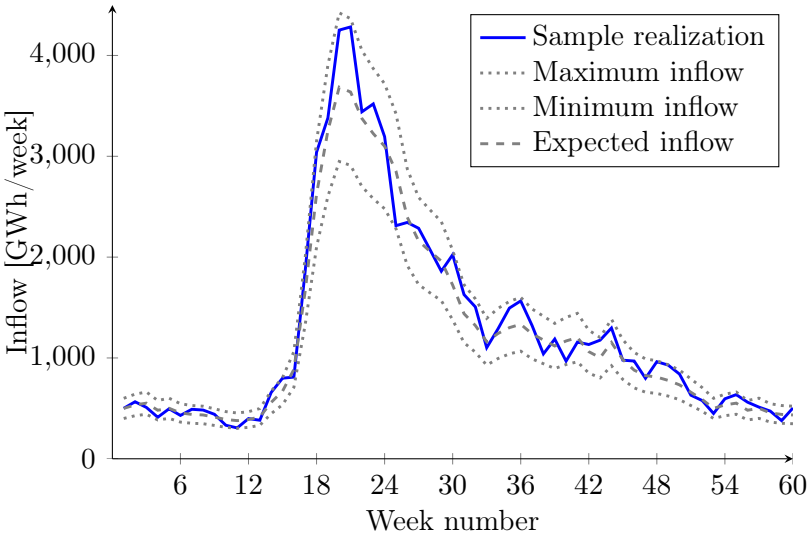

Figure 3.5: Expected inflow in Sweden with upper and lower bounds with and uncertainty of θ^I=0.2.

To describe the uncertainty set on the form of Equation (2.2) the $\boldsymbol{W}$-matrix and $\boldsymbol{h}$-vector takes the following form:

$$\boldsymbol{W} = \begin{bmatrix} 1 & 0 & \cdots & 0 \\ -1 & 0 & \cdots & 0 \\ -I^*_{1,1}(1-\theta^I) & 1 & \cdots & 0 \\ I^*_{1,1}(1+\theta^I) & -1 & \cdots & 0 \\ \vdots & \vdots & \ddots & \vdots \\ -PG^*_T(1-\theta^{PG}) & 0 & \cdots & 1 \\ PG^*_T(1+\theta^{PG}) & 0 & \cdots & -1 \end{bmatrix}, \quad \boldsymbol{h} = \begin{bmatrix} 1 \\ -1 \\ 0 \\ 0 \\ \vdots \\ 0 \\ 0 \end{bmatrix}.$$

There are two rows for each random parameter, so the length of $\boldsymbol{W}$ and $\boldsymbol{h}$ is twice the total amount of uncertain parameters, $2k$.

Moment estimation To incorporate dependencies between the different uncertain parameters the the moment matrix, $\boldsymbol{M} = \mathbb{E}(\boldsymbol{\xi}\boldsymbol{\xi}^\top)$ must be specified. As the uncertainties are modelled to be mutually independent the covariance between two parameters is zero. The covariance of a random variable with it self is the variance of the random variable, and the diagonal elements of $\boldsymbol{M}$ therefore include variance terms.

$$\mathbf{M} = \begin{bmatrix} I^*_{1,1} \times I^*_{1,1} + Var(I_{1,1}) & I^*_{1,1} \times I^*_{1,2} & \cdots & I^*_{1,1} \times PG^*_T \\ I^*_{1,2} \times I^*_{1,1} & I^*_{1,2} \times I^*_{1,2} + Var(I_{1,2}) & \cdots & I^*_{1,2} \times PG^*_T \\ \vdots & \vdots & \ddots & \vdots \\ PG^*_T \times I^*_{1,1} & PG^*_T \times I^*_{1,2} & \cdots & PC^*_T \times PG^*_T + Var(PG_T) \end{bmatrix}.$$

The uncertain parameters are uniformly distributed between the bounds defined in 3.11. By using basic probability theory the variance of the uncertain inflow can be expressed as:

$$\text{Var}(I_{ti}) = \frac{I^*_{ti}\theta^I}{3}$$

In the case of mutually independent random parameters, the conditional expectations reduce to unconditional expectations, and the matrix $\boldsymbol{M}_t \in \mathbb{R}^{k \times k^t}$ in Problem $\mathcal{P}^U$ defined in Section 2.2 is divided in two parts. The first $k^t \times k^t$ submatrix is an identity matrix, and the last $(k^t + 1), \ldots, k$ rows contain the expected value of the parameter in the first column, and zero for the remainder of the columns.

It should be noted that approximating the uncertain parameters to be mutually independent is a major simplification. Inflow in one week is correlated to the inflow last week and the inflow in neighboring areas. When it comes to fuel prices, the probability space is dependent on global demand for energy, structural bottlenecks in the supply chain and technological development (O. Lofsnes and E. Torgnes, personal communication, May 4, 2012). Furthermore, there exists some correlation between the coal and the gas price which are not reflected in the model. However the LDR framework supports such dependencies, and changes need only be made in the $\boldsymbol{M}$ and $\boldsymbol{M}_t$ matrices to incorporate this. An approach that incorporates the underlying stochastic processes, is to perform a sampling procedure of the random variables as is done in Rocha and Kuhn (2012) by using for example Monte Carlo sampling.

Variables The number of decisions to be taken in each time period, n_t, consists of the generation g_{tji} and transmission b_{tl}. In our case this means that $n_t = J \times A + L = 46$, and according to the matrix formulation introduced in Section 1, the decision variables $\boldsymbol{x}_t$ can be written as one vector:

$$\boldsymbol{x}_t^\top = (g_{t,1,1}, g_{t,1,2}, \ldots, g_{t,j,i}, \ldots, g_{t,J,A}, b_{t1}, \ldots, b_{t,l}, \ldots, b_{t,L})$$

Recall that the decision variables are linear functions of the uncertain parameters, such that $\boldsymbol{x}_t = \boldsymbol{x}_t(\boldsymbol{\xi}^t) = \boldsymbol{X}_t\boldsymbol{\xi}^t$. The entries of the matrix $\boldsymbol{X}_t \in \mathbb{R}^{n_t \times k^t}$ are the decision variables of the LDR problem, together with the support variables $\boldsymbol{\Lambda}_t \in \mathbb{R}^{m_t \times 2k}$ and $\boldsymbol{\Gamma}_t \in \mathbb{R}^{n_t \times 2k}$.

Parameters All cost coefficients have linear dependence on the observation history $\boldsymbol{\xi}^t$, that is $\boldsymbol{c}_t = \boldsymbol{c}_t(\boldsymbol{\xi}^t) = \boldsymbol{C}_t\boldsymbol{\xi}^t$. The matrix $\boldsymbol{C}_t \in \mathbb{R}^{n_t \times k^t}$ contains the deterministic cost-coefficients in the first column, as $\boldsymbol{\xi}_1 = 1$. The elements of $\boldsymbol{c}_t$ which are dependent on the observation histories are the costs of coal-, and gas-fueled generation. As none of the stage-t constraints are affected by future decisions, $\boldsymbol{A}_{ts} = 0$ for all $t \leq s$. The elements of the $\boldsymbol{A}_{ts}$-matrix are zero when $s < t$ except for the rows corresponding to the water balance constraints. In these constraints the hydro-generation variables from the previous periods are involved. The right-hand- side matrix, $\boldsymbol{B}_t \in \mathbb{R}^{m_t \times k^t}$, consist of elements only in the first column, with an exception again of the water-balance constraints. As the sum of inflows up to time t is present in the right hand side of these constraints, there are non-zero elements in the columns corresponding to the inflows for past time periods.

Problem size In each time period there are A power balance constraints shown in (3.2), and $2 \times H$ water balance constraints shown in Equations (3.3) and (3.4). There are also $2 \times (J \times A + L)$ constraints securing variable bounds, seen in Equations (3.5) – (3.7). This means that the number of constraints in each period, m_t, is equal to 102 except for in the last period where there are $2 \times H$ additional water balance constraints securing the end reservoir level. The matrix $\boldsymbol{A}_{ts} \in \mathbb{R}^{m_t \times n_t}$ is then a 102×46 matrix.

The size of the generation planning problem grows quickly with the number of uncertain parameters revealed in each period, k_t. In addition to the program with uncertainty in both inflow and fuel prices described in this section, primal and dual versions of two simplified models are developed to attain computational convenience. One of the simplified models have deterministic fuel prices and stochastic inflow, whereas the other has stochastic fuel prices and deterministic inflow. The number of uncertain parameters are then reduced to $k_t = 3$ and $k_t = 2$ respectively. The sizes of these simplified programs are shown in Table 3.6, and it can be seen that the problem size is substantially reduced with fewer uncertain parameters.

Stage aggregation Implementation of stage aggregation reduce the dimensions of many of the parameter- and variable-matrices in the problem due to the reduc-

Table 3.6: Dual and primal problem size for different number of uncertain parameters.

	k_t=5		k_t= 3		k_t=2	
	Primal	Dual	Primal	Dual	Primal	Dual
# variables	5 670 372	6 171 108	3 410 436	3 712 224	2 280 468	2 482 782
# constraints	2 639 142	2 639 142	1 590 594	1 590 594	1 066 320	1 066 320

tion in k_t. When for example the planning horizon is 60 weeks and the number of macroperiods is 10, $\boldsymbol{\xi}^{t_s} = \boldsymbol{\xi}^{t_s+1} =, \ldots, = \boldsymbol{\xi}^{t_s+5}$. As mentioned in Section 2.4, k_t equals zero as long as t is not the first time period in a macro period. Many of the matrices has to be adapted to the new information structure. The water balance constraints within each macroperiod uses the *expected* inflow scenario to plan the decisions, and when new information arrives when a new macroperiod is entered, the decisions are readjusted according to actual inflow. When it comes to planning with uncertain fuel prices, the decision maker bases all decisions within one macroperiod s on the fuel price observed at t_s. Figure 3.6 show how the problem size increases linearly with the number of macroperiods. Stage aggregation with 60 macroperiods equals the problem without stage aggregation.

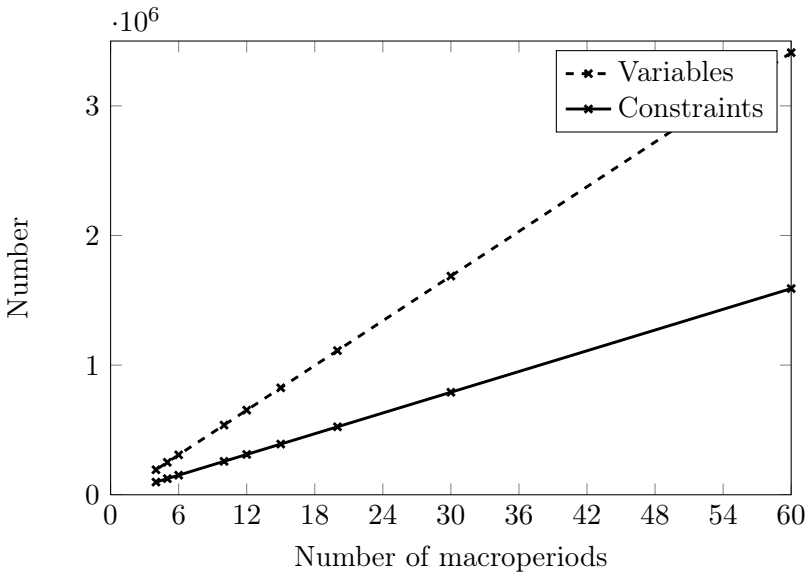

Figure 3.6: Primal problem size with uncertainty in inflow at different number of macroperiods.

4 Computational results

Numerical results are obtained using the solver package XPRESS^{MP} and the implementation is written in the MOSEL language. A linux cluster of 2.4 GHz processors with 24Gb RAM is used to run the models.

We investigate the effect of uncertainty in inflow and fuel prices on the accuracy and runtime of the LDR model. To assess the value of adaptivity in the LDR model, we compare the optimal value of the primal program with that of a deterministic planning program. We also investigate the effect of uncertainty on power prices and reservoir levels. Stage aggregation is implemented as a means to reduce complexity, and the appropriateness of this is evaluated.

Unless all uncertainties are explicitly defined as non-zero, we have used the "simplified" models with either only fuel price uncertainty or only inflow uncertainty.

4.1 Suitability of the LDR approach

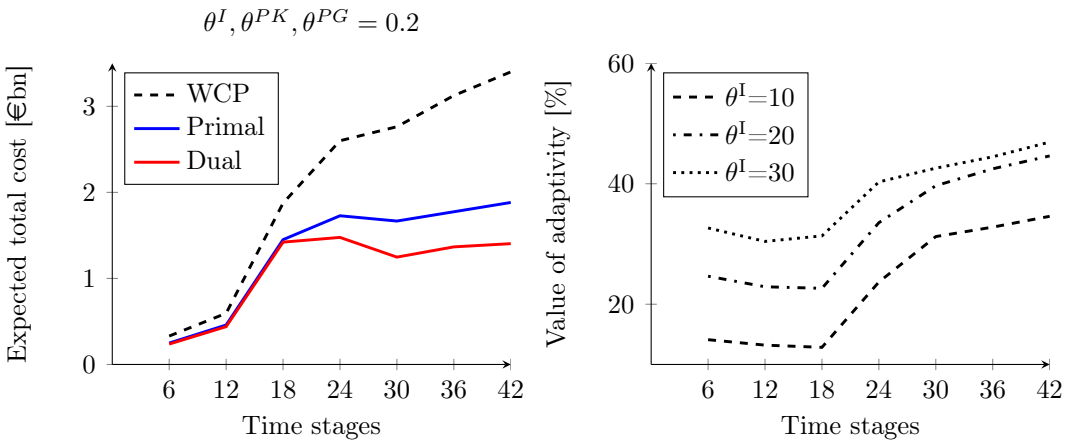

Figure 4.1: Impact of uncertainties on accuracy and the value of adaptivity for different planning horizons.

From Figure 4.1, we see that with increasing planning horizon, the cumulative cost increases. The primal and dual LDR problems define the bounds for the optimal objective value for the exact problem. The gap between these bounds is the Δ defined in Equation (2.4), and increases with the planning horizon, indicating a loss of accuracy with increased planning horizon. Worst case planning (WCP) is an appropriate way to model a decision maker that has to commit to a generation strategy at the start of the planning horizon without being able to adapt to

observations. As reservoir limits must be guaranteed, worst case for a generation planner corresponds to the lowest possible inflow scenario. The WCP expected total cost was calculated using generation targets from the deterministic solution with low inflow scenario, and is depicted in Figure 4.1. The primal LDR approximation defines a feasible solution to the uncertain generation planning problem, and the expected total cost can therefore be compared to the expected total cost from worst case planning. We define the value of adaptivity to be the additional value of being able to adapt to observations. This value is calculated as the difference between the WCP objective and primal LDR objective, as a percentage of the worst case objective.

The runtime for the programs with both inflow and fuel price uncertainty is in the order of two days for just 42 time periods, which is unacceptable for a real operation.

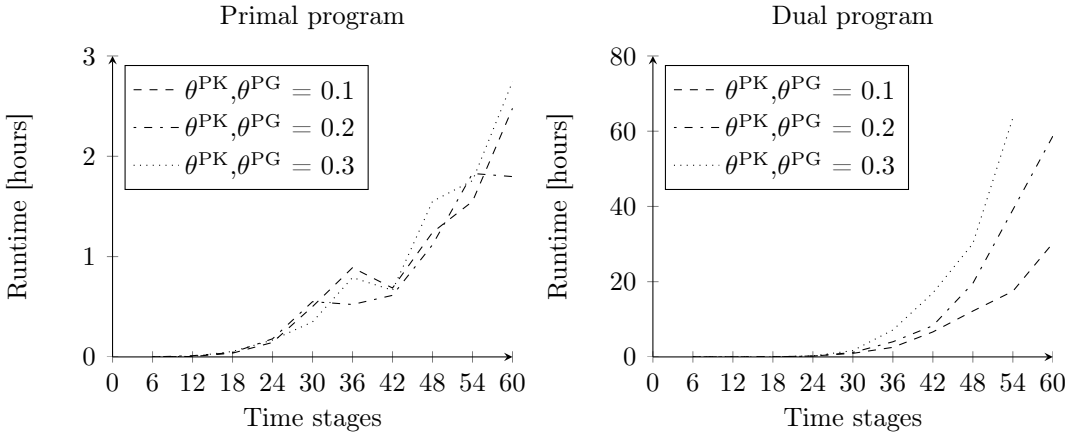

Figure 4.2: Runtimes for primal and dual problem with fuel price uncertainty.

Figure 4.2 show the runtimes for the primal and dual program with different fuel price uncertainty levels and planning horizons. As expected, the runtime follows a quadratic shape, increasing with the number of time stages. The runtimes of the dual program are many times longer than the primal program. This is because the fuel price uncertainty affects the objective function in the primal program while it affects the constraints in the dual program reducing the feasible region. The characteristics are reversed for the programs with inflow uncertainty. For the primal program the inflow uncertainty affects the constraints making this the more time consuming program to solve. The inflow uncertainty affects the constraints in the primal program and this is why the primal runtime is longer in this case.

Figures 4.3 and 4.4 show how inflow uncertainty and fuel price uncertainty affect the Δ for different planning horizons. In general, the accuracy of the LDR solution

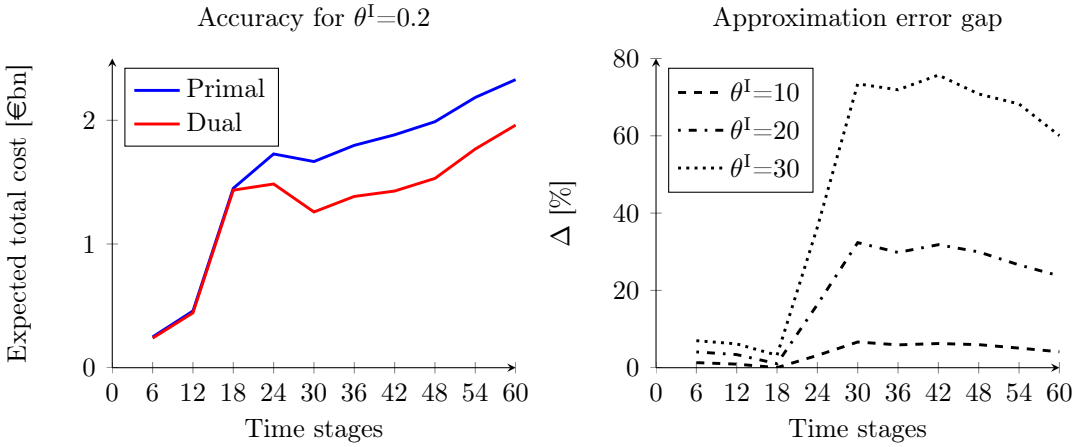

Figure 4.3: Impact of inflow uncertainty and planning horizon on approximation accuracy.

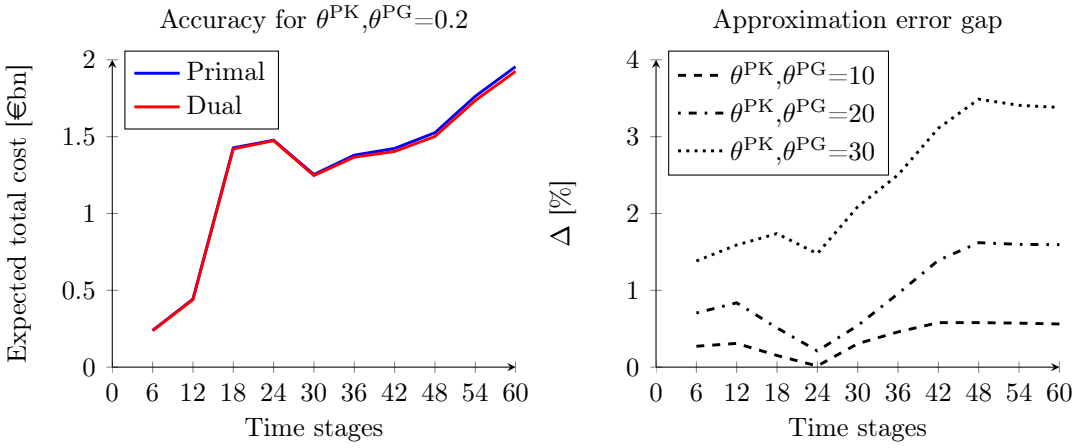

Figure 4.4: Impact of fuel price uncertainty and planning horizon on approximation accuracy.

decreases as the time horizon and uncertainty level increase. Inflow uncertainty has a considerably larger impact on the solution accuracy than fuel price uncertainty. As the Nordic region is dominated by hydropower, it is no surprise that the problem is more sensitive to uncertainty in inflow than that of fuel prices. We notice a substantial increase in the approximation error gap in Figure 4.3 as the planning horizon exceeds 18 time stages. This coincides with the timing of the spring flood as seen in Figure 3.3. When the inflow suddenly rises, so does the spread of possible inflow scenarios, and it becomes harder to generate good linear decision rules that encapsulate this spread. This is also the reason why the Δ decreases if the planning horizon lasts longer than until after the summer season. A Δ of close to 60% when there is inflow uncertainty is much higher than in the case of only fuel price uncertainty, when the Δ is only 3.5% for the planning horizon of 60 weeks. Even though optimality cannot be guaranteed, the value of adaptivity is more than 40%, and this shows that the LDR approach provides a solution that is substantially better than that of a WCP approach.

4.2 Power prices

In optimization theory, the shadow price of a constraint corresponds to the marginal cost of tightening the constraint, or the marginal utility of relaxing the constraint. In the power balance constraints, the shadow price is the marginal cost of consuming one more unit of power, and this can be interpreted as the power price in €/MWh under the assumption of perfect competition. Figure 4.5 shows the average power prices generated by the model at different inflow uncertainty levels. This is compared to the system price in the actual planning period 2008–2009. From this we can see that the power prices increase as the level of uncertainty increases. As the uncertainty level increases, it becomes necessary for the planner to hold back on the free hydro-generation to ensure that end reservoir constraints are met. More expensive generation must then be used, resulting in increased power prices. The prices also become more volatile at high levels of θ^I. The actual system price in the modelling period is not the best comparison however, as the fuel prices in this period were abnormally high, and the model uses fuel prices which are the average between the years 2000–2010. The level of the power price from the model is similar to real power prices, and the uncertainty level of $\theta^I = 0.3$ gives the best fit power price with the actual system price. This indicates that the actual inflow uncertainty is even higher than 0.3.

Figure 4.6 shows the power prices for the different areas at the uncertainty level $\theta^I = 0.3$. Sweden and Norway have relatively stable power prices throughout the planning period, while Finland and Denmark have more volatile prices. The reason

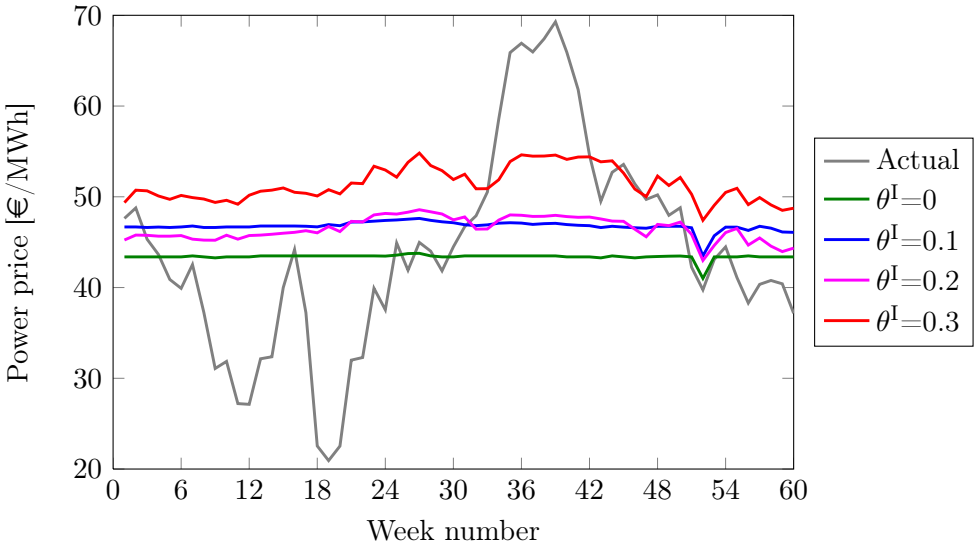

Figure 4.5: Average area prices for different values of uncertainties compared to the actual system price.

for this is the relative amount of hydropower available in each country. Whereas Sweden and Norway has the majority of their demand for power covered by hydro, Denmark and Finland are more dependent on coal and gas-fueled generator types. This demonstrates the advantage of having the ability to store water in between periods, and not being so exposed to fluctuations in the fuel prices.

The impact of fuel price uncertainty on the power price forecast is limited in Norway, Finland, and Sweden. Here, the power prices rise only around 1%, while in Denmark the change is more notable as seen in Table 4.1. This is again because Denmark is more dependent on thermal generators and has strong connections to Germany. Table 4.1 shows the maximum and minimum percentage change in power prices during the planning horizon when the fuel price uncertainty is increased from zero to $\theta^{PK}, \theta^{PG} = 0.2$.

Table 4.1: Effect of increasing fuel price uncertainty from 0 to 0.2 on power prices.

	NO	SE	FI	DK
Max change [%]	1.29	1.27	1.29	33.36
Min change [%]	1.29	1.27	1.29	-20.15

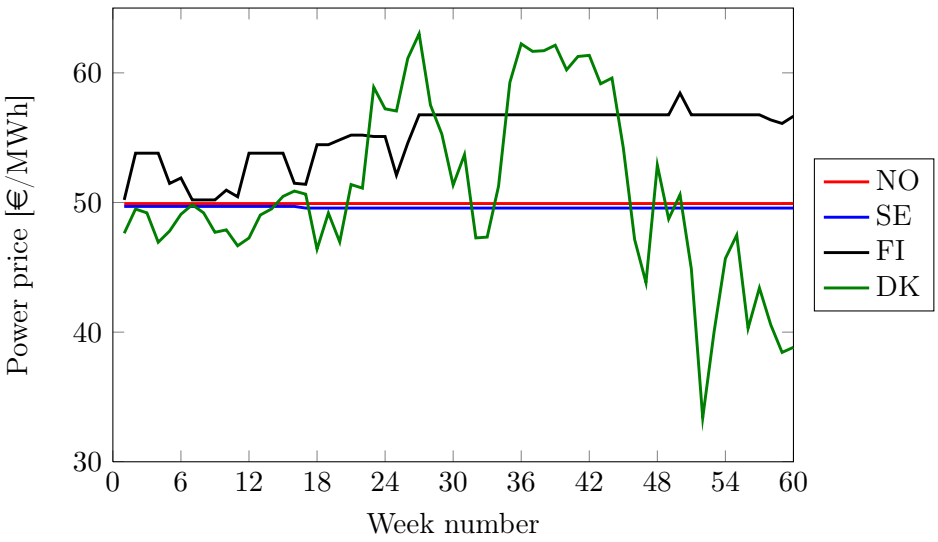

Figure 4.6: Price forecasts in the different areas with $\theta^I = 0.3$.

4.3 Reservoir levels

By combining the decision rules resulting from the optimization process with actual scenarios, we can analyze how the realization of different scenarios affects actual decisions. The reservoir level is a good indication of this effect, as it illustrates how the available water is distributed for different scenarios. Figure 4.7 shows the reservoir levels in all hydro-producing areas as a function of time, and the historic average reservoir levels are plotted alongside. Extreme inflow scenarios with $\theta^I = 0.3$ are shown in the graphs. We see that the high and average inflow scenarios coincide well with the historic averages. When the lowest possible inflow scenario occurs, the realized reservoir levels are lower than average. In Finland the reservoir levels do not coincide that well with the historic average. This is possibly because the actual reservoir capacity is significantly lower than in Sweden and Norway.

The target end reservoir is shown as a dotted line, and when inspecting the actual end values, we can see that this target is met if the expected inflow scenario occurs. However, in the case of low inflow, the end reservoir is below the target. This is because the decision maker assumed expected inflow in the last period.

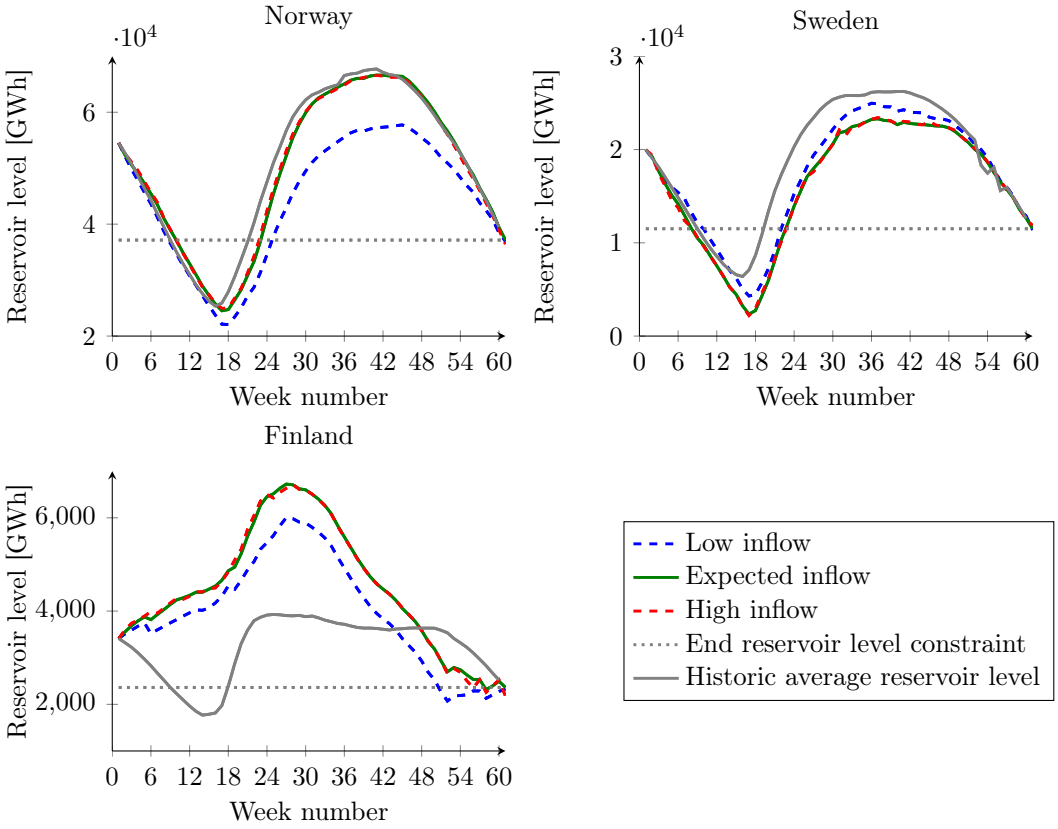

Figure 4.7: Reservoir levels in all areas for different inflow scenarios, plotted together with the historic averages.

4.4 Complexity reduction

Problem reduction Before XPRESS^{MP} calls the optimizer, a pre-solve is automatically performed to reduce the size of the problem. Table 4.2 shows that the number of variables and constraints in the primal program with uncertain inflow was more than halved by this size reduction. This shows a potential for more efficient formulation of the problem so that less variables and constraints are needed, which in turn would lead to a reduction in runtime. When the inflow uncertainty is set to zero, the problem reduces to a deterministic one, drastically reducing the problem size.

Stage aggregation To reduce the size of the problem, stage aggregation was implemented for the LDR model of 60 weeks. Figure 4.8 shows how the number of macroperiods affect the runtime of the model and the objective value. As expected,

Table 4.2: Complexity reduction of automatic pre-solve by XPRESS^{MP}.

		θ^I=0.2		θ^I=0	
	Original size	After presolve	Reduction [%]	After presolve	Reduction [%]
# variables	3 410 436	1 587 009	53	2217	99.93
# constraints	1 590 594	536 208	66	597	99.96

the runtimes becomes shorter as the number of macroperiods is reduced. The complexity reduction of stage aggregation comes with a loss of accuracy, shown by the objective value in the figure. As the number of macroperiods approaches the number of actual periods, the objective value converges from above to the objective value for the porblem without stage aggragation. As stage aggregation provides less flexible decision rules, the objective value of the problem with stage aggregation provides an upper bound to the objective value of the LDR problem without stage aggregation. Figure 3.6 indicates that an approximation based on six macroperiods provides a reasonably accurate solution as the objective value is only 1.2% higher than the optimal objective value with 60 time stages. The reduction in runtime is close to 70%, and this indicates the advantage of applying stage aggregation. The runtime is eight hours, which is still fairly long for a generation planner.

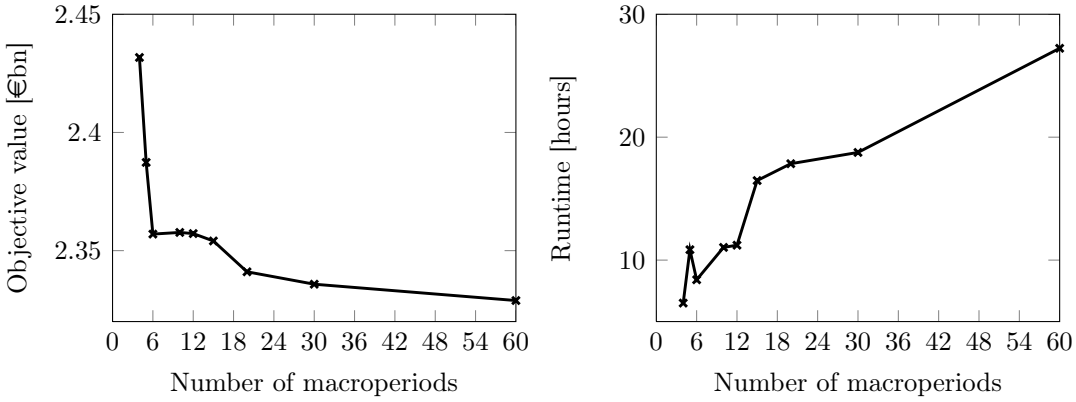

Figure 4.8: Objective values and runtimes for the primal program with $\theta^I = 0.2$ with different number of macroperiods.

Figure 4.9 shows how the decision rules are applied to actual scenarios to produce generation targets for hydro production in Norway when the inflow is at either of the extreme scenarios. When the inflow scenario is low, the generation targets are adjusted to account for less available water. The opposite is true in the case of high inflow where the same decision rules result in higher generation targets due to the observation history of high inflows. The generation targets using the decision

rules from the model with six macroperiods, are very similar to that of no stage aggregation. This shows how decision rules resulting from the model using stage aggregation produce good quality generation targets. The decision rules from the stage aggregation model result in the same generation targets for both scenarios for the duration of the first macroperiod. No new information is revealed during the first macroperiod, and the the generation targets do therefore not adapt to actual inflow scenario.

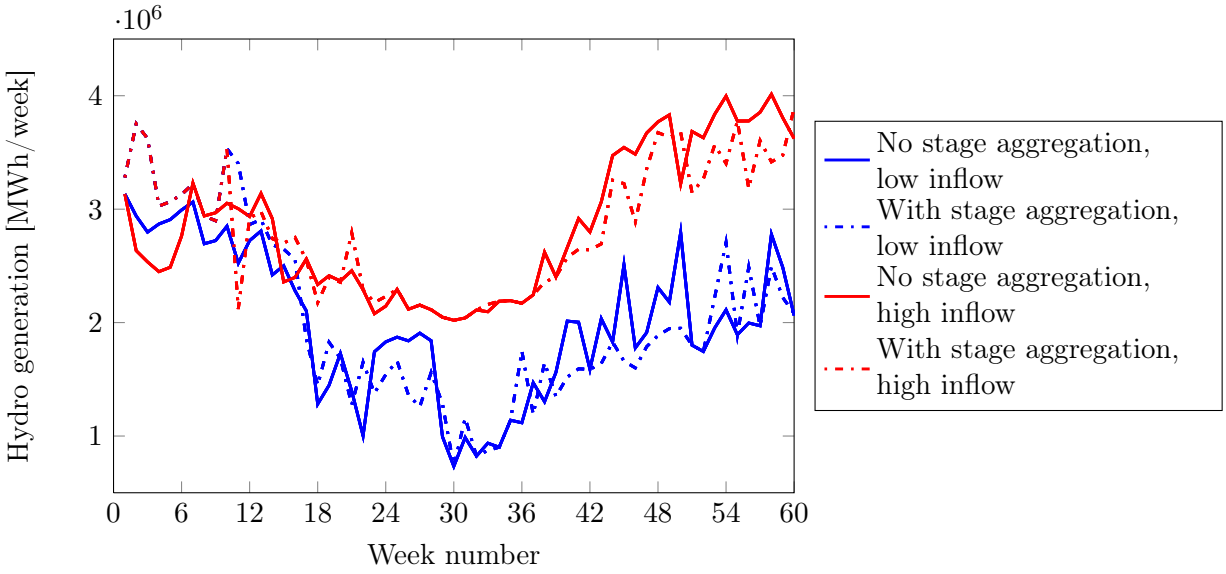

Figure 4.9: Hydro production in Norway for $\theta^I = 0.2$ with and without the use of stage aggregation of six macroperiods.

5 Conclusion

In this thesis, a multi-stage stochastic generation planning problem for the Nordic region is studied. By restricting the decision rules to only those which are linear in the observation history of uncertain parameters, the original intractable program is transformed into a tractable one. The linear decision rule restriction is also applied to the dual version of the original problem, and these programs are implemented in XPRESS^{MP}. Power prices and reservoir levels from the models coincides well with actual data from the planning period. The difference between the objective values of the primal and the dual programs define Δ, which is the upper bound on the approximation error imposed by the LDR approach.

We find that Δ increases as the planning horizon and the uncertainty levels increase, and that inflow uncertainty has a substantially larger impact on Δ than uncertainty in fuel prices. In fact, for a planning horizon of 60 weeks and inflow uncertainty of 30 %, Δ is close to 60%. This indicates a potentially high optimality gap of the LDR solution. However, as the optimal value of the excact problem is unattainable, comparison to other tractable approximations is important. When compared to WCP, the flexibility available from using the LDR approach is substantial. Other stochastic modelling methods traditionally used for comparable problems quickly grows to inconvenient dimensions, and involve demanding scenario generation. In conclusion, we can say that the LDR approach generates good feasible solutions at reasonable efforts, thus making it an attractive approach for the stochastic generation planning problem.

References

A. Atamturk and M. Zhang. Two-stage robust network flow and design under demand uncertainty. *Operations Research-Baltimore*, 55(4):662–673, 2007.

R. Bellman. Dynamic programing. *Princeton, New Jersey*, 1957.

A. Ben-Tal, A. Goryashko, E. Guslitzer, and A. Nemirovski. Adjustable robust solutions of uncertain linear programs. *Mathematical Programming*, 99(2):351–376, 2004.

A. Ben-Tal, B. Golany, A. Nemirovski, and J.P. Vial. Retailer-supplier flexible commitments contracts: a robust optimization approach. *Manufacturing & Service Operations Management*, 7(3):248–271, 2005.

X. Chen, M. Sim, P. Sun, and J. Zhang. A linear decision-based approximation approach to stochastic programming. *Operations Research*, 56(2):344–357, 2008.

M. Dyer and L. Stougie. Computational complexity of stochastic programming problems. *Mathematical Programming*, 106(3):423–432, 2006.

P.J. Goulart, E.C. Kerrigan, and D. Ralph. Efficient robust optimization for robust control with constraints. *Mathematical Programming*, 114(1):115–147, 2008.

E. Guslitser. *Uncertainty-immunized solutions in linear programming*. PhD thesis, Technion-Israel Institute of Technology, 2002.

H. Heitsch and W. Römisch. Scenario tree modeling for multistage stochastic programs. *Mathematical Programming*, 118(2):371–406, 2009.

J. L. Higle. Stochastic programming: Optimization when uncertainty matters. *Tutorials in Operations Research*, pages 30–53, 2005.

M. Kaut and S.W. Wallace. Evaluation of scenario-generation methods for stochastic programming. *Pacific Journal of Optimization*, 3(2):257–271, 2007.

D. Kuhn, W. Wiesemann, and A. Georghiou. Primal and dual linear decision rules in stochastic and robust optimization. *Mathematical Programming*, 130: 1–33, 2009.

D. Kuhn, W. Wiesemann, and A. Georghiou. The decision rule approach to optimisation under uncertainty: Methodology and applications in operations management. Department of Computing, Imperial College London, 2011.

J. Lundgren, M. Rönnqvist, and P. Varbrand. *Optimization*. Studentlitteratur, 2010.

M. V. F. Pereira and L. Pinto. Multi-stage stochastic optimization applied to energy planning. *Mathematical Programming*, 52(1):359–375, 1991.

C. Revelle, E. Joeres, and W. Kirby. The linear decision rule in reservoir management and design: 1, development of the stochastic model. *Water Resources Research*, 5(4):767–777, 1969.

P. Rocha and D. Kuhn. Multistage stochastic portfolio optimisation in deregulated electricity markets using linear decision rules. *European Journal of Operational Research*, 216(2):397 – 408, 2012.

A. Shapiro and A. Nemirovski. On complexity of stochastic programming problems. *Continuous Optimization*, 99:111–146, 2005.

O. Wolfgang, A. Haugstad, B. Mo, A. Gjelsvik, I. Wangensteen, and G. Doorman. Hydro reservoir handling in norway before and after deregulation. *Energy*, 34 (10):1642–1651, 2009.

Appendix A

In this section we give a short description of the attached files. The files are also available at the following webpage: http://folk.ntnu.no/vefring.

Data.xls gives all the data and data sources used in the modelling.

matrices.m is a MATLAB-script creating all the matrices used in the formulation.

CreateMoselCode.m is a MATLAB-script taking the matrices created in matrices.m as input, and performing the necessary matrix manipulations in order to format the problem codes in both primal and dual versions.

PrimalTemplate.mos is the MOSEL-code with the primal problem calling the optimizer. It includes the text-file with MOSEL-code created by CreateMoselCode.m.

DualTemplate.mos is the MOSEL-code with the dual problem calling the optimizer.

DataW_T60.txt and TidsDataW_T60.txt are datafiles included by PrimalTemplate.mos and DualTemplate.mos

NordiskDeterministisk.mos is the deterministic version of the generation planning program.